CHEMISTRY
A EUROPEAN JOURNAL

DOI: 10.1002/chem.201000294

Neutral Penta- and Hexacoordinate Silicon(IV) Complexes Containing Two Bidentate Ligands Derived from the α-Amino Acids (*S*)-Alanine, (*S*)-Phenylalanine, and (*S*)-*tert*-Leucine

Smaranda Cota, Matthias Beyer, Rüdiger Bertermann, Christian Burschka, Kathrin Götz, Martin Kaupp, and Reinhold Tacke*[a]

Abstract: The neutral hexacoordinate silicon(IV) complex **6** (SiO_2N_4 skeleton) and the neutral pentacoordinate silicon(IV) complexes **7**–**11** (SiO_2N_2C skeletons) were synthesized from $Si(NCO)_4$ and $RSi(NCO)_3$ (R = Me, Ph), respectively. The compounds were structurally characterized by solid-state NMR spectroscopy (**6**–**11**), solution NMR spectroscopy (**6** and **10**), and single-crystal X-ray diffraction (**8** and **11** were studied as the solvates **8**·CH_3CN and **11**·C_5H_{12}·0.5 CH_3CN, respectively). The silicon(IV) complexes **6** (octahedral Si-coordination polyhedron) and **7**–**11** (trigonal-bipyramidal Si-coordination polyhedra) each contain two bidentate ligands derived from an α-amino acid: (*S*)-alanine, (*S*)-phenylalanine, or (*S*)-*tert*-leucine. The deprotonated amino acids act as monoanionic (**6**) or as mono- and dianionic ligands (**7**–**11**). The experimental investigations were complemented by computational studies of the stereoisomers of **6** and **7**.

Keywords: amino acids · coordination chemistry · coordination modes · silicon · stereochemistry

Introduction

In general, the chemistry of higher-coordinate silicon(IV) complexes with bidentate mono- and dianionic ligands is well explored.[1] Very little is known, however, about higher-coordinate silicon compounds that contain bidentate ligands derived from α-amino acids. Some years ago, we reported the first examples of this type, compounds **1**–**5**.[2,3] These zwitterionic λ^5Si-silicates contain two identical bidentate dianionic ligands derived from glycine, (*S*)-alanine, (*S*)-valine, (*S*)-*tert*-leucine, or (*S*)-phenylalanine. Compounds **1**–**5** have been synthesized by using "the zwitterion trick",[4] that is, the pentacoordinate (formally negatively charged) silicon atom has been incorporated into a molecular framework that also contains a tetracoordinate (formally positively charged) nitrogen atom. We have now succeeded in synthesizing a series of structurally different neutral higher-coordinate silicon(IV) complexes that also contain bidentate ligands derived from α-amino acids, namely, compounds **6**–**11**. To the best of our knowledge, compound **6** is the first hexacoordinate silicon(IV) complex with ligands derived from an α-amino acid, (*S*)-alanine. Contrary to the pentacoordinate silicon(IV) complexes **1**–**5** (two dianionic chelate ligands), compound **6** contains two monoanionic chelate ligands and thus represents a neutral species. Quite remarkably, in the neutral pentacoordinate silicon(IV) complexes **7**–**11**, both of these different coordination modes are realized; one of the two chelate ligands acts as a bidentate dianionic ligand (analogous to compounds **1**–**5**), whereas the other one acts as a bidentate monoanionic ligand (analogous to compound **6**). The studies presented herein were performed as part of our systematic investigations on higher-coordinate silicon compounds (for recent publications, see ref. [5]; for other recent publications dealing with higher-coordinate silicon compounds, see ref. [6]).

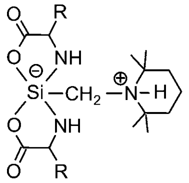

	1	2	3	4	5
R	H	Me	*i*Pr	*t*Bu	Bn

1 – **5**

---

[a] Dipl.-Chem. S. Cota, Dipl.-Chem. M. Beyer, Dr. R. Bertermann, Dr. C. Burschka, Dr. K. Götz, Prof. Dr. M. Kaupp, Prof. Dr. R. Tacke
Universität Würzburg, Institut für Anorganische Chemie
Am Hubland, 97074 Würzburg (Germany)
Fax: (+49) 931-31-84609
E-mail: r.tacke@uni-wuerzburg.de

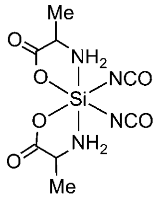

6

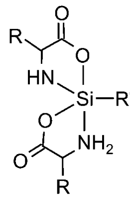

7−11

	7	**8**	**9**	**10**	**11**
R	Me	Me	Bn	Bn	*t*Bu
R'	Me	Ph	Me	Ph	Ph

Results and Discussion

Syntheses: Compounds **6**–**11** were synthesized according to Scheme 1 by the treatment of tetra(cyanato-*N*)silane,[7] tri(cyanato-*N*)methylsilane,[7] and tri(cyanato-*N*)phenylsilane[8] with two molar equivalents of trimethylsilyl (*S*)-*N*-(trimethylsilyl)alaninate,[9] trimethylsilyl (*S*)-*N*-(trimethylsilyl)phenylalaninate,[9] and trimethylsilyl (*S*)-*N*-(trimethylsilyl)-*tert*-leucinate,[9] respectively. The syntheses were performed at −70 to −20 °C (**6**–**8**, **10**), at −30 to −20 °C (**9**), and at −45 to −20 °C (**11**). All syntheses were carried out in acetonitrile. Compound **6**–**11** were isolated as colorless crystalline solids (yields: 51 (**6**), 56 (**7**), 34 (**8**), 48 (**9**), 57 (**10**), and 49 % (**11**)). The moderate yields of compounds **6**–**11** can be explained by the occurrence of a side reaction of the respective disilylated amino acid [$Me_3SiOC(O)CHRN(SiMe_3)H$] (R = Me, Bn, *t*Bu), which leads to the formation of an oligopeptide of the type $Me_3SiOC(O)CHR[N(SiMe_3)C(O)CHR]_nN(SiMe_3)H$. The oligopeptide formation involves the elimination of trimethylsilanol (Me_3SiOH), which can undergo a condensation reaction to yield hexamethyldisiloxane ($Me_3SiOSiMe_3$) and water. Both the oligopeptide and the disiloxane could be detected as by-products in the synthesis of **6**–**8** (NMR spectroscopy studies). The water formed in this side reaction may be the proton source that could explain the existence of the NH_2 group of the bidentate monoanionic O,N ligands of **6**–**11**. It is of interest to note that the oligopeptide formation from $Me_3SiOC(O)CHRN(SiMe_3)H$ (R = Me, Bn, *t*Bu) only occurs upon addition of the (cyanato-*N*)silanes ($Si(NCO)_4$, $MeSi(NCO)_3$, and $PhSi(NCO)_3$, respectively); NMR spectroscopy studies performed with trimethylsilyl (*S*)-*N*-(trimethylsilyl)alaninate that was stored without solvent or as a solution in dichloromethane at room temperature over a period of three weeks did not show any evidence for oligopeptide formation.

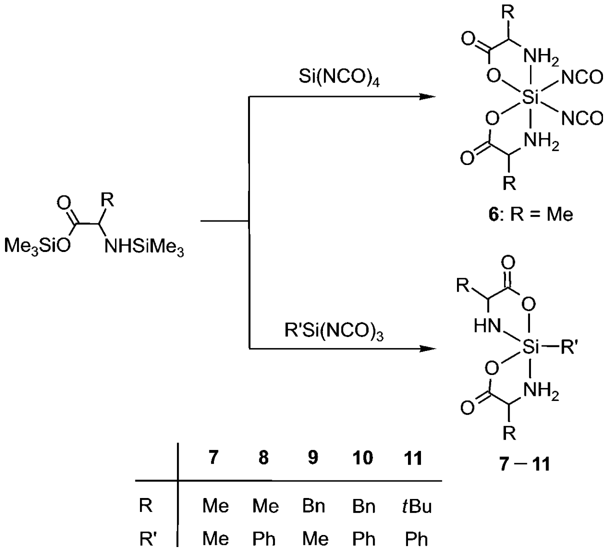

	7	8	9	10	11
R	Me	Me	Bn	Bn	*t*Bu
R'	Me	Ph	Me	Ph	Ph

Scheme 1. Syntheses of compounds **6**–**11**.

The identities of **6**–**11** were established by elemental analyses (C, H, N), single-crystal X-ray diffraction studies (**8** and **11** were studied as the solvates **8**•CH_3CN and **11**•C_5H_{12}•0.5 CH_3CN), and VACP/MAS NMR experiments (^{13}C, ^{15}N, ^{29}Si). Owing to their poor solubility in organic solvents and/or decomposition upon dissolution, compounds **7**–**9** and **11** could not be characterized by NMR spectroscopy in solution, whereas studies of **6** and **10** in solution ([D_6]DMSO) were possible.

Crystal structure analyses: Compounds **6**, **7**, **8**•CH_3CN, **9**, **10**, and **11**•C_5H_{12}•0.5 CH_3CN were structurally characterized by single-crystal X-ray diffraction. The crystal data and the experimental parameters used for the crystal structure analyses are given in Table 1. The molecular structures of **6**–**11** in the crystal are shown in Figures 1–6; selected bond lengths and angles are given in the figure legends. All compounds studied form intermolecular N−H···O hydrogen bonds that lead to the formation of infinite three-dimensional (**6**, **7**, **8**•CH_3CN) or two-dimensional (**9**) networks, or to infinite one-dimensional chains (**10**, **11**•C_5H_{12}•0.5 CH_3CN) in the crystal.[10]

As can be seen from Figure 1, the Si-coordination polyhedron of **6** is a somewhat distorted octahedron. The two monodentate cyanato-*N* ligands and the two oxygen ligand atoms O1 and O1A each occupy *cis* positions, whereas the two amino nitrogen atoms N1 and N1A are in *trans* positions. The maximum deviations from the ideal 90 and 180° angles amount to 4.57° (N1-Si-N2, 94.57(5)°) and 7.92° (N1-Si-N1A, 172.08(8)°), respectively. The Si−O distances (1.7995(10) Å) of **6** are similar to the axial Si−O bond lengths of the distorted trigonal-bipyramidal Si-coordination polyhedra of compounds **1**–**5** (1.8058(14)–1.8524(13) Å) and **7**–**11** (1.7871(14)–1.8038(11) Å). The Si−N1 and Si−N1A bond lengths of **6** (1.8857(11) Å) are significantly shorter than the axial Si−N distances of compounds **7**–**10** (1.9658(17)–1.9932(14) Å) (same coordination mode). The Si−N distances of the Si−NCO moieties of **6** are similar to those of other hexacoordinate silicon(IV) complexes with cyanato-*N* ligands.[5b,11] The same holds true for the N-C-O angles of the Si−NCO groups, whereas the Si-N2-C1 and Si-N2A-C1A angles (146.33(13)°) of **6** are significantly smaller than the Si-N-C angles of the Si−NCO groups of other hexacoordinate silicon(IV) complexes (151.62(12)–169.77(12)°).[5b,11]

As can be seen from Figures 2–5, the Si-coordination polyhedra of **7**, **8**•CH_3CN, **9** (two molecules in the asymmetric unit), and **10** are distorted trigonal bipyramids, with

Table 1. Crystallographic data for compounds **6**, **7**, **8**$\cdot$$CH_3CN$, **9**, **10**, and **11**$\cdot$$C_5H_{12}\cdot0.5\,CH_3CN$.

	6	**7**	**8**$\cdot CH_3CN$	**9**	**10**	**11**$\cdot C_5H_{12}\cdot 0.5\,CH_3CN$
formula	$C_8H_{12}N_4O_6Si$	$C_7H_{14}N_2O_4Si$	$C_{14}H_{19}N_3O_4Si$	$C_{19}H_{22}N_2O_4Si$	$C_{24}H_{24}N_2O_4Si$	$C_{24}H_{41.5}N_{2.5}O_4Si$
M_r	288.31	218.29	321.41	370.48	432.54	457.19
T [K]	100(2)	193(2)	193(2)	193(2)	100(2)	100(2)
λ ($Mo_{K\alpha}$) [Å]	0.71073	0.71073	0.71073	0.71073	0.71073	0.71073
crystal system	tetragonal	orthorhombic	orthorhombic	orthorhombic	monoclinic	tetragonal
space group (no.)	$P4_12_12$ (92)	$P2_12_12_1$ (19)	$P2_12_12_1$ (19)	$P2_12_12_1$ (19)	$P2_1$ (4)	$I4_1$ (80)
a [Å]	7.69110(10)	7.6563(6)	8.5016(7)	6.5828(6)	6.6931(4)	17.9928(2)
b [Å]	7.69110(10)	10.9386(9)	11.1129(13)	23.3334(18)	13.5206(9)	17.9928(2)
c [Å]	20.1180(4)	12.4438(12)	17.5068(16)	24.524(2)	11.9450(8)	16.1878(4)
β [°]	90	90	90	90	103.534(2)	90
V [Å^3]	1190.04(3)	1042.16(16)	1654.0(3)	3766.9(6)	1050.94(12)	5240.65(15)
Z	4	4	4	8	2	8
ρ_{calcd} [g cm^{-3}]	1.609	1.391	1.291	1.307	1.367	1.159
μ [mm^{-1}]	0.230	0.218	0.162	0.151	0.147	0.121
F(000)	600	464	680	1568	456	1992
crystal size [mm]	$0.2\times0.1\times0.1$	$0.5\times0.5\times0.5$	$0.5\times0.5\times0.5$	$0.5\times0.4\times0.3$	$0.36\times0.1\times0.1$	$0.3\times0.1\times0.03$
2θ range [°]	5.68–61.00	7.28–56.16	5.92–56.08	4.82–55.96	3.50–57.04	3.20–66.30
index ranges	$-10\leq h\leq10$	$-10\leq h\leq9$	$-11\leq h\leq10$	$-8\leq h\leq8$	$-8\leq h\leq8$	$-27\leq h\leq27$
	$-7\leq k\leq10$	$-11\leq k\leq14$	$-14\leq k\leq13$	$-29\leq k\leq30$	$-18\leq k\leq16$	$-27\leq k\leq27$
	$-25\leq l\leq28$	$-16\leq l\leq16$	$-23\leq l\leq18$	$-26\leq l\leq32$	$-16\leq l\leq15$	$-24\leq l\leq24$
collected reflns	9842	6283	8202	27644	30894	102915
unique reflns	1812	2512	3983	8931	5062	10016
R_{int}	0.0357	0.0220	0.0349	0.0414	0.0520	0.0475
restraints	0	0	0	0	1	41
parameters	97	139	211	489	289	304
S[a]	1.146	1.061	1.072	0.977	1.029	1.077
weight parameters a/b[b]	0.0405/0.3333	0.0530/0.0676	0.0630/0.0000	0.0455/0.0000	0.0264/0.3140	0.0604/1.9965
$R1$[c] [$I>2\sigma(I)$]	0.0307	0.0301	0.0445	0.0328	0.0269	0.0373
$wR2$[d] (all data)	0.0816	0.0801	0.1028	0.0755	0.0667	0.1032
Flack parameter	0.02(14)	0.00(12)	−0.01(13)	0.03(7)	0.05(7)	0.00(6)
max/min residual electron density [e Å^{-3}]	+0.358/−0.214	+0.235/−0.151	+0.345/−0.209	+0.276/−0.178	+0.266/−0.192	+0.494/−0.438

[a] $S=\{\Sigma[w(F_o^2-F_c^2)^2]/(n-p)\}^{0.5}$; n = number of reflections; p = number of parameters. [b] $w^{-1}=\sigma^2(F_o^2)+(aP)^2+bP$, with $P=[\max(F_o^2,0)+2F_c^2]/3$. [c] $R1=\Sigma\,||F_o|-|F_c||/\Sigma|F_o|$. [d] $wR2=\{\Sigma[w(F_o^2-F_c^2)^2]/\Sigma[w(F_o^2)^2]\}^{0.5}$.

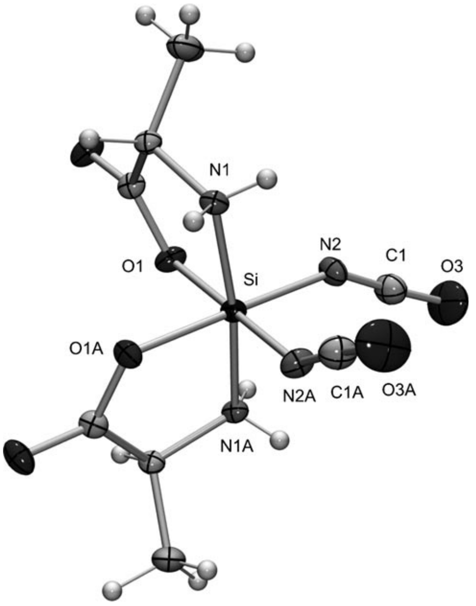

Figure 1. Molecular structure of **6** in the crystal (probability level of displacement ellipsoids 50 %). Selected bond lengths [Å] and angles [°]: Si–O1 1.7995(10), Si–N1 1.8857(11), Si–N2 1.8026(12); O1-Si-O1A 88.27(7), O1-Si-N1 86.51(5), O1-Si-N1A 87.80(5), O1-Si-N2 89.77(5), O1-Si-N2A 176.83(5), N1-Si-N1A 172.08(8), N1-Si-N2 94.57(5), N1-Si-N2A 90.92(5), N2-Si-N2A 92.29(8), Si-N2-C1 146.33(13), N2-C1-O3 176.99(19).

Berry distortions (transition trigonal bipyramid→square pyramid; pivot atom C1) of 20.7 (**7**), 23.8 (**8**$\cdot CH_3CN$), 21.2 (**9**, molecule **I**), 12.0 (**9**, molecule **II**), and 19.6 % (**10**).[10]

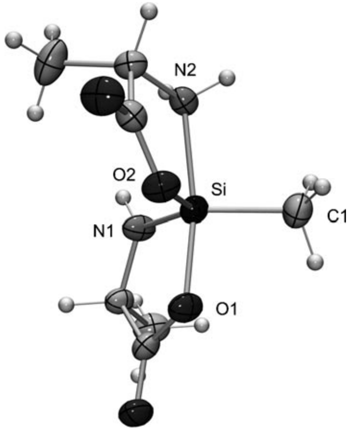

Figure 2. Molecular structure of **7** in the crystal (probability level of displacement ellipsoids 50 %). Selected bond lengths [Å] and angles [°]: Si–O1 1.7910(13), Si–O2 1.7118(11), Si–N1 1.6901(14), Si–N2 1.9932(14), Si–C1 1.8401(18); O1-Si-O2 86.63(6), O1-Si-N1 87.69(6), O1-Si-N2 167.64(6), O1-Si-C1 95.29(8), O2-Si-N1 123.85(7), O2-Si-N2 83.57(6), O2-Si-C1 111.63(8), N1-Si-N2 91.52(6), N1-Si-C1 124.52(9), N2-Si-C1 95.31(8).

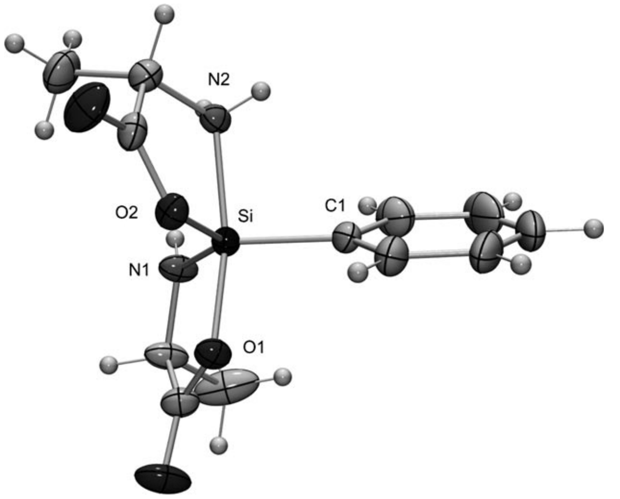

Figure 3. Molecular structure of **8** in the crystal of **8**$\cdot$$CH_3CN$ (probability level of displacement ellipsoids 50%). Selected bond lengths [Å] and angles [°]: Si−O1 1.7871(14), Si−O2 1.7082(14), Si−N1 1.6885(17), Si−N2 1.9658(17), Si−C1 1.854(2); O1-Si-O2 86.98(7), O1-Si-N1 87.68(7), O1-Si-N2 168.25(7), O1-Si-C1 96.12(8), O2-Si-N1 125.90(9), O2-Si-N2 84.22(7), O2-Si-C1 110.61(9), N1-Si-N2 91.18(8), N1-Si-C1 123.49(10), N2-Si-C1 94.27(8).

The two axial positions of **7**–**10** are occupied by the O1 oxygen atom and the N2 nitrogen atom (NH_2 group), whereas the O2 oxygen atom, the N1 nitrogen atom (NH group), and the C1 carbon atom are found in the three equatorial sites. Thus, compounds **7**–**10** have non-VSEPR (VSEPR = valence-shell electron pair repulsion) structures because only one of the two oxygen atoms occupies an axial position. This phenomenon is not yet understood, but computational studies of **7** also demonstrated the non-VSEPR structure to be more stable than the isomeric structure with the two oxygen ligand atoms in the axial sites (see the Computational Studies section). The experimental finding, however, should not be overestimated; the energy differences between the various isomers of **7** are rather small, and the different structures observed for compounds **7**–**10** (non-VSEPR structures) and **11** (VSEPR structure) might be the result of crystal-packing effects.

The sums of the equatorial bond angles of **7**–**10** amount to 360° and the axial O1-Si-N2 angles are in the range 167.64(6)–170.55(6)°. The equatorial O2-Si-N1, O2-Si-C1, and N1-Si-C1 angles are in the ranges 120.56(6)–125.90(9), 110.61(9)–115.63(7), and 123.36(8)–124.52(9)°, respectively.

The axial Si−O1 distances of compounds **7**–**10** (1.7871(14)–1.8038(11) Å) are somewhat longer than the equatorial Si−O2 bond lengths (1.7042(10)–1.7220(12) Å) and similar to the axial Si−O distances of the zwitterionic compounds **1**–**5** (1.8058(14)–1.8356(19) Å). The equatorial Si−N1 bond lengths of **7**–**10** (1.6885(17)–1.7114(13) Å) are substantially shorter than the axial Si−N2 distances (1.9658(17)–1.9932(14) Å) and similar to the equatorial Si−N bond lengths of **1**–**5** (1.7087(17)–1.725(3) Å). The equatorial Si−C1 distances of compounds **7**–**10** (1.8401(18)–1.8654(18) Å) are significantly shorter than the equatorial Si−C bond lengths of the zwitterions **1**–**5** (1.906(3)–1.9274(18) Å).

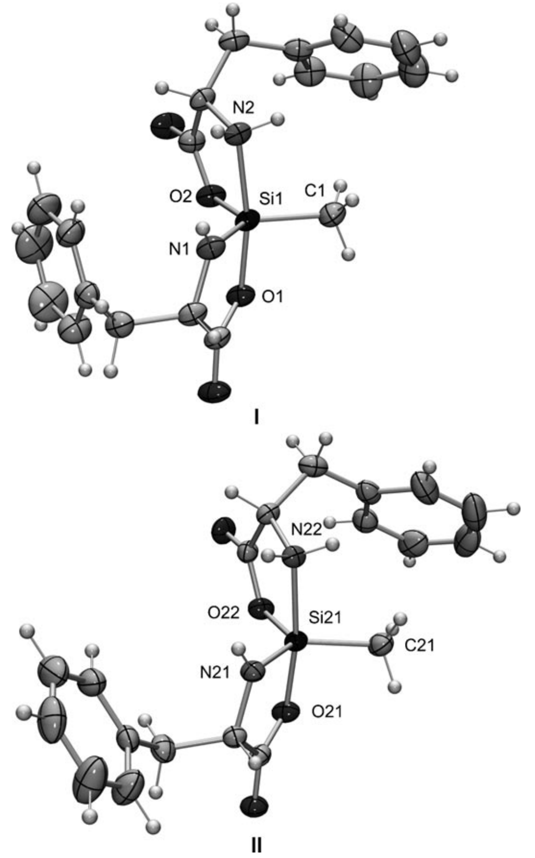

Figure 4. Molecular structures of the two crystallographically independent molecules (**I** and **II**) of **9** in the crystal (probability level of displacement ellipsoids 50%). Selected bond lengths [Å] and angles [°] of molecule **I**: Si1−O1 1.8038(11), Si1−O2 1.7207(12), Si1−N1 1.7052(15), Si1−N2 1.9731(13), Si1−C1 1.8654(18); O1-Si1-O2 87.85(6), O1-Si1-N1 86.63(6), O1-Si1-N2 169.01(6), O1-Si1-C1 96.42(7), O2-Si1-N1 124.53(7), O2-Si1-N2 85.19(5), O2-Si1-C1 112.11(7), N1-Si1-N2 90.32(6), N1-Si1-C1 123.36(8), N2-Si1-C1 94.07(7). Selected bond lengths [Å] and angles [°] of molecule **II**: Si21−O21 1.7995(10), Si21−O22 1.7220(12), Si21−N21 1.7114(13), Si21−N22 1.9823(12), Si21−C21 1.8581(17); O21-Si21-O22 87.38(5), O21-Si21-N21 87.39(5), O21-Si21-N22 170.55(6), O21-Si21-C21 93.88(7), O22-Si21-N21 120.56(6), O22-Si21-N22 85.21(5), O22-Si21-C21 115.63(7), N21-Si21-N22 91.34(5), N21-Si21-C21 123.80(7), N22-Si21-C21 94.61(7).

As in the case of compounds **7**–**10**, the Si-coordination polyhedron of **11**$\cdot$$C_5H_{12}$$\cdot$0.5 CH_3CN is a distorted trigonal bipyramid (Figure 6; Berry distortion = 26.8%),[10] however, the coordination mode of the bidentate monoanionic O,N ligand of **11** is quite different. The oxygen atoms O1 and O2 of **11** occupy the two axial positions, whereas in the case of compounds **7**–**10** only one of the two oxygen atoms of the ligand are found in an axial position. Therefore, in contrast to compounds **7**–**10**, the structure of **11** is compatible with the VSEPR concept. The O1-Si-O2 angle of **11** amounts to 164.88(4)° and the sum of the equatorial bond angles is 359.9°. The axial Si−O1 (1.8199(8) Å) and Si−O2 (1.7876(8) Å) bond lengths are similar to the axial Si−O distances of compounds **1**–**5** (1.8058(14)–1.8356(19) Å) and **7**–

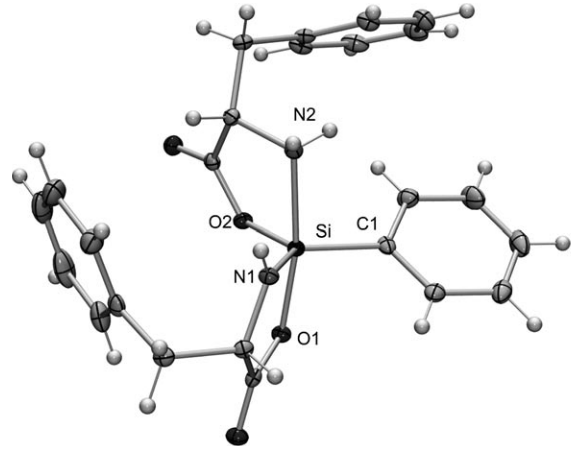

Figure 5. Molecular structure of **10** in the crystal (probability level of displacement ellipsoids 50%). Selected bond lengths [Å] and angles [°]: Si–O1 1.8004(9), Si–O2 1.7042(10), Si–N1 1.6991(12), Si–N2 1.9677(11), Si–C1 1.8583(13); O1-Si-O2 88.35(5), O1-Si-N1 87.11(5), O1-Si-N2 169.43(5), O1-Si-C1 95.04(5), O2-Si-N1 123.98(5), O2-Si-N2 84.66(5), O2-Si-C1 111.65(5), N1-Si-N2 90.24(5), N1-Si-C1 124.37(6), N2-Si-C1 94.90(5).

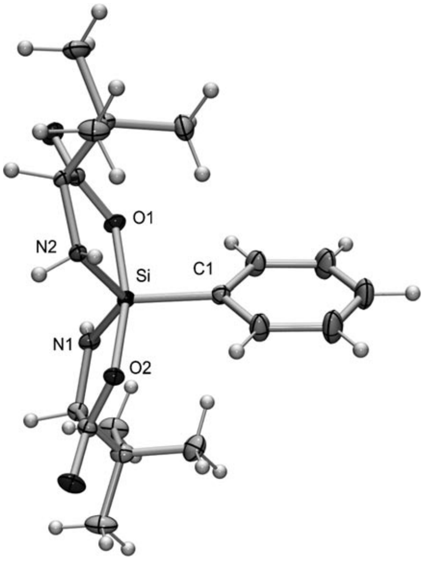

Figure 6. Molecular structure of **11** in the crystal of $\mathbf{11}\cdot C_5H_{12}\cdot 0.5\,CH_3CN$ (probability level of displacement ellipsoids 50%). Selected bond lengths [Å] and angles [°]: Si–O1 1.8199(8), Si–O2 1.7876(8), Si–N1 1.7040(9), Si–N2 1.8842(9), Si–C1 1.8659(11); O1-Si-O2 164.88(4), O1-Si-N1 86.48(4), O1-Si-N2 84.91(4), O1-Si-C1 96.70(4), O2-Si-N1 90.28(4), O2-Si-N2 84.86(4), O2-Si-C1 97.59(4), N1-Si-N2 124.96(4), N1-Si-C1 121.45(5), N2-Si-C1 113.53(4).

10 (1.7871(14)–1.8038(11) Å). The equatorial Si–N1 (NH group) bond length of **11** is similar to the equatorial Si–N (NH group) distances of compounds **1**–**5** (1.7087(17)–1.725(3) Å) and **7**–**10** (1.6885(17)–1.7114(13) Å), and the equatorial Si–N2 (NH_2 group) bond length (1.8842(9) Å) is somewhat shorter than the axial Si–N (NH_2 group) distances of **7**–**10** (1.9658(17)–1.9932(14) Å).

Computational studies: To obtain more information about the stereochemistry of compounds **6**–**11**, structure optimizations and frequency calculations for the eight possible stereoisomers of the hexacoordinate silicon(IV) complex **6** and for the six possible stereoisomers of the pentacoordinate silicon(IV) complex **7** were performed. In these studies, compound **7** also served as a model system for the related pentacoordinate silicon compounds **8**–**11**. The computational studies were performed with the TURBOMOLE 5.10[12] program package at the BP86[13]/SVP[14] level of theory.

The configurations of the eight possible stereoisomers of **6**, the diastereoisomers **6a**–**6h**, and their calculated relative energies are shown in Figure 7. The maximum energy difference amounts to 42.5 kJ mol^{-1}. The three isomers with both NH_2 groups in the *trans* positions (2.5 (**6a**), 0 (**6b**) and 14.2 kJ mol^{-1} (**6g**)) are the most stable species, and the configuration of **6a** corresponds to the experimentally established structure of **6** in the crystal (Figure 1). Based on these results, it is assumed that the two most stable isomers **6a** and **6b** represent the two species (molar ratio, ca. 1:1) detected by solution NMR spectroscopy (see below).

The configurations of the six possible stereoisomers of **7**, the diastereoisomers **7a**–**7f**, and their calculated relative energies are shown in Figure 8. The maximum energy difference amounts to 12.5 kJ mol^{-1}. The configuration of **7a** corresponds to the experimentally established structures of **7**

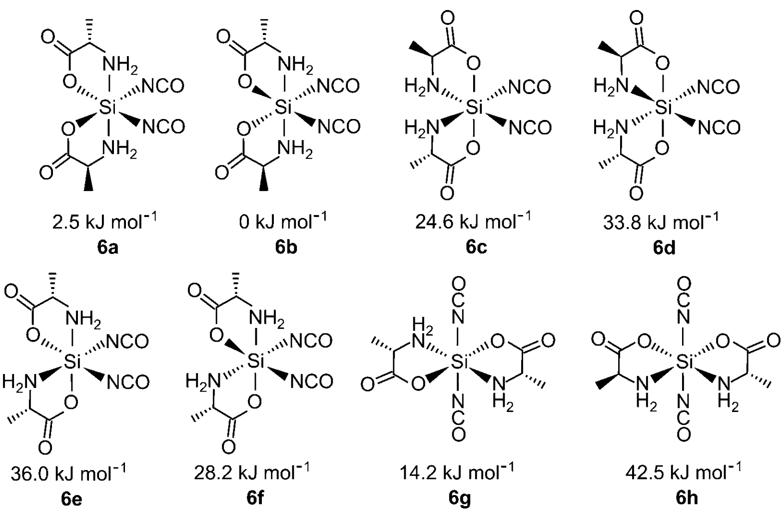

Figure 7. Configurations and calculated relative energies for the eight possible stereoisomers of compound **6**, the diastereoisomers **6a**–**6h**.

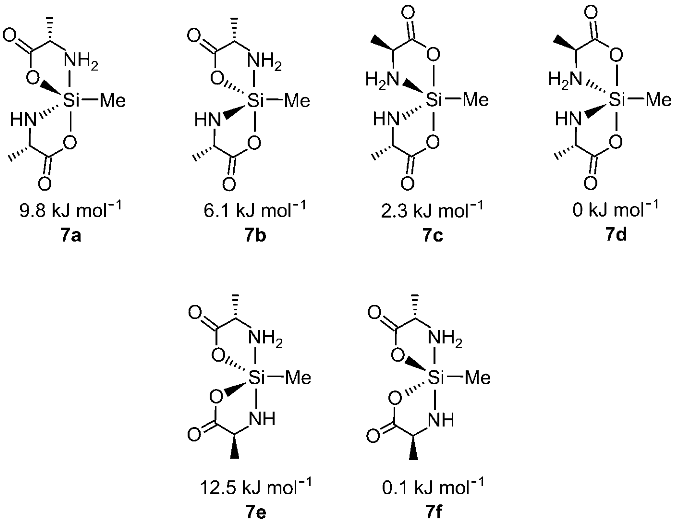

9.8 kJ mol^{-1} **7a**; 6.1 kJ mol^{-1} **7b**; 2.3 kJ mol^{-1} **7c**; 0 kJ mol^{-1} **7d**; 12.5 kJ mol^{-1} **7e**; 0.1 kJ mol^{-1} **7f**

Figure 8. Configurations and calculated relative energies for the six possible stereoisomers of **7**, the diastereoisomers **7a**–**7f**.

and **8** (studied as **8**•CH_3CN) in the crystal, whereas **7c** corresponds to the structure of **11** in the crystal of **11**•C_5H_{12}•0.5 CH_3CN (Figure 6). The configuration of **7b** corresponds to the crystal structures of **9** and **10** (Figures 4 and 5). As the maximum energy difference observed for **7a**–**7f** is rather small, it is not surprising that three different configurations, namely, **7a**, **7b**, and **7c**, are realized in the crystal structures of the pentacoordinate silicon(IV) complexes studied. Due to this small energy difference, a configurational assignment for the two species of **10** (molar ratio, ca. 1:1.3) detected by solution NMR spectroscopy is not possible (see below).

NMR spectroscopic studies in the solid state and in solution: Compounds **6**–**11** were characterized by solid-state VACP/MAS NMR spectroscopy (^{13}C, ^{15}N, ^{29}Si). The spectra obtained are compatible with the results of the crystal structure analyses. The isotropic ^{29}Si chemical shifts ($\delta = -187.4$ (**6**), −84.4 (**7**), −96.0 (**8**), −87.9/−85.5 (**9**; two crystallographically independent molecules), −98.5 (**10**), −92.3 ppm (**11**)) clearly indicate the presence of hexacoordinate (**6**) and pentacoordinate (**7**–**11**) silicon atoms. The hexacoordinate silicon(IV) complex **6** and the pentacoordinate silicon(IV) complex **10** were also studied by solution NMR spectroscopy (^{1}H, ^{13}C, ^{15}N, ^{29}Si) in [D$_6$]DMSO. The data obtained indicate the presence of more than one species in solution in both cases. The isotropic ^{29}Si chemical shifts clearly indicate the existence of two hexacoordinate species in the case of **6** ($\delta = -191.9/-191.8$ ppm; molar ratio, ca. 1:1 ($c = 20$ mM)) and the existence of two pentacoordinate species in the case of **10** ($\delta = -99.1/-97.7$ ppm; molar ratio, ca. 1:1.3 ($c = 72$ mM)). The two species of **6** in solution are most likely to be the diastereoisomers **6a** and **6b**, whereas a configurational assignment for the two isomers of **10** in solution is not possible (see the Computational Studies section). Due to their poor solubility and/or decomposition in [D$_6$]DMSO, compounds **7**–**9** and **11** could not be characterized in solution.

Conclusion

With the synthesis of **6**, we have succeeded in preparing the first hexacoordinate silicon(IV) compound with ligands derived from an α-amino acid. In this neutral hexacoordinate silicon(IV) complex, (*S*)-alanine behaves as a bidentate monoanionic O,N ligand. For the first time, this particular coordination mode has also been realized for pentacoordinate silicon compounds, namely, the neutral silicon(IV) complexes **7**–**11**. In these compounds, however, the respective α-amino acids ((*S*)-alanine, (*S*)-phenylalanine, and (*S*)-*tert*-leucine) also act as bidentate dianionic O,N ligands. On the basis of these results, the synthesis of a whole variety of novel penta- and hexacoordinate silicon(IV) complexes with mono- and/or dianionic bidentate O,N ligands that derive from natural and unnatural α-amino acids should be possible. Future studies are needed to explore the potential of this chemistry. In this context, it should be mentioned that compounds **7** and **9** and other related silicon(IV) complexes with an SiMe moiety and two bidentate ligands derived from different α-amino acids might be of interest for practical applications. The hydrolysis of these compounds would lead to the formation of the respective free α-amino acids and methylsilanetriol ($MeSi(OH)_3$), a silicon food supplement of long-standing use in humans that is currently being discussed as a potential drug for the improvement of bone and other connective tissue health.[15] Compounds **7** and **9** and related silicon(IV) complexes might also serve as silicon food supplements or as pro-drugs for methylsilanetriol.

Experimental Section

General procedures: All syntheses were carried out under dry argon. The organic solvents used were dried and purified according to standard procedures and stored under dry nitrogen. Melting points were determined with a Büchi Melting Point B-540 apparatus using samples in sealed capillaries. The ^{1}H, ^{13}C, ^{15}N, and ^{29}Si NMR spectroscopy studies in solution were performed at 23 °C on a Bruker Avance 500 (^{1}H, 500.1 MHz; ^{13}C, 125.8 MHz; ^{15}N, 50.7 MHz; ^{29}Si, 99.4 MHz) or on a Bruker DRX-300 NMR spectrometer (^{15}N, 30.4 MHz; **6** only). [D$_6$]DMSO was used as the solvent. Chemical shifts (ppm) were determined relative to internal [D$_5$]DMSO (^{1}H, $\delta = 2.49$ ppm), internal [D$_6$]DMSO (^{13}C, $\delta = 39.5$ ppm), external formamide (^{15}N, $\delta = -268.0$ ppm), or external TMS (^{29}Si, $\delta = 0$ ppm). Analysis and assignment of the ^{1}H NMR data was supported by 2D ^{1}H–^{1}H, ^{13}C–^{1}H, ^{15}N–^{1}H, and ^{29}Si–^{1}H correlation experiments. Assignment of the ^{13}C NMR data was supported by DEPT 135 and the above-mentioned ^{13}C–^{1}H correlation experiments. Solid-state ^{13}C, ^{15}N, and ^{29}Si VACP/MAS NMR spectra were recorded at 22 °C on a Bruker DSX-400 NMR spectrometer with bottom layer rotors of ZrO_2 (diameter, 7 mm) containing approximately 300 mg of sample (^{13}C, 100.6 MHz; ^{15}N, 40.6 MHz; ^{29}Si, 79.5 MHz; external standard, TMS (^{13}C and ^{29}Si, $\delta = 0$ ppm) or glycine (^{15}N, $\delta = -342.0$ ppm); spinning rate, 6–7 kHz; contact time, 2 (^{13}C), 1–3 (^{15}N), or 3–5 ms (^{29}Si); 90° ^{1}H transmitter pulse length, 3.6 μs; repetition time, 4 s).

Synthesis of 6: Trimethylsilyl (*S*)-*N*-(trimethylsilyl)alaninate (1.17 g, 5.01 mmol) was added in a single portion at −70 °C to a stirred solution of tetra(cyanato-*N*)silane (490 mg, 2.50 mmol) in acetonitrile (15 mL), and the mixture was then kept undisturbed at −20 °C for 3 d. The resulting colorless, crystalline solid was isolated by filtration, washed with cold (0 °C) *n*-pentane (3×10 mL), and dried in vacuo (0.8 mbar, 20 °C, 6 h); yield, 365 mg (1.27 mmol, 51 %). M.p. >230 °C (decomp). The following solution NMR data refer to two isomers (molar ratio, ca. 1:1): ^{1}H NMR (c = 20 mM): δ = 1.32/1.33 (d, 6H, ^3J(H,H) = 7.3 Hz; CH_3), 3.48–3.57/3.57–3.66 (m, 2H; CH), 6.58–6.69 and 7.10–7.28 ppm (m, 4H; NH_2); ^{13}C NMR (c = 20 mM): δ = 16.4/16.8 (CH_3), 49.81/49.83 (CH), 118.7 (br "s"; NCO), 171.2/171.4 ppm (CO); ^{15}N NMR (30.4 MHz; c, 20 mM)): δ = −322.0 ppm (NH_2, ^{15}N signals for the two isomers not resolved), ^{15}N signals for the NCO moieties not detected; ^{29}Si NMR (c = 20 mM): δ = −191.9/−191.8 ppm; ^{13}C VACP/MAS NMR: δ = 18.7 (CH_3), 51.0 (asymmetric "d"; CH),[16] 122.8 (br "d"; NCO),[16] 177.0 ppm (CO); ^{15}N VACP/MAS NMR: δ = −315.9 (NCO), −314.2 ppm (NH_2); ^{29}Si VACP/MAS NMR: δ = −187.4 ppm (br "s");[16] elemental analysis calcd (%) for $C_8H_{12}N_4O_6Si$ (288.29): C 33.33, H 4.20, N 19.43; found: C 33.5, H 4.3, N 19.3.

Synthesis of 7: Trimethylsilyl (*S*)-*N*-(trimethylsilyl)alaninate (1.17 g, 5.01 mmol) was added in a single portion at −70 °C to a stirred solution of tri(cyanato-*N*)methylsilane (423 mg, 2.50 mmol) in acetonitrile (10 mL), and the mixture was then kept undisturbed at −20 °C for 3 d. The resulting colorless crystalline solid was isolated by filtration, washed with cold (0 °C) *n*-pentane (3×10 mL), and dried in vacuo (0.8 mbar, 20 °C, 24 h); yield, 306 mg (1.40 mmol, 56 %). M.p. >288 °C (decomp); ^{13}C VACP/MAS NMR: δ = 4.6 ($SiCH_3$), 16.9 (CCH_3), 22.7 (CCH_3), 50.1 (asymmetric "d"; CH),[16] 52.3 (asymmetric "d"; CH),[16] 176.1 (CO), 180.0 ppm (CO); ^{15}N VACP/MAS NMR: δ = −325.8 (NH or NH_2), −324.1 ppm (NH or NH_2); ^{29}Si VACP/MAS NMR: δ = −84.4 ppm (asymmetric "d");[16] elemental analysis calcd (%) for $C_7H_{14}N_2O_4Si$ (218.28): C 38.52, H 6.46, N 12.83; found: C 38.5, H 6.4, N 12.8.

Synthesis of 8: Trimethylsilyl (*S*)-*N*-(trimethylsilyl)alaninate (1.17 g, 5.01 mmol) was added in a single portion at −70 °C to a stirred solution of tri(cyanato-*N*)phenylsilane (578 mg, 2.50 mmol) in acetonitrile (10 mL), and the mixture was then kept undisturbed at −20 °C for 3 d. The resulting colorless crystalline solid was isolated by filtration, washed with cold (0 °C) *n*-pentane (2×10 mL), and dried in vacuo (0.1 mbar, 60 °C, 8 h); yield, 240 mg (856 μmol, 34 %). M.p. >360 °C (decomp); ^{13}C VACP/MAS NMR: δ = 15.5 (CH_3), 22.1 (CH_3), 50.3 (br asymmetric "d"; CH),[16] 52.7 (asymmetric "d"; CH),[16] 128.2, 130.6, and 138.5 (C_6H_5), 173.9 (CO), 177.4 ppm (CO); ^{15}N VACP/MAS NMR δ = −323.2 (NH or NH_2), −320.3 ppm (NH or NH_2); ^{29}Si VACP/MAS NMR: δ = −96.0 ppm (br asymmetric "d");[16] elemental analysis calcd (%) for $C_{12}H_{16}N_2O_4Si$ (280.36): C 51.41, H 5.75, N 9.99; found: C 50.7, H 5.7, N 9.7.

Synthesis of 9: Trimethylsilyl (*S*)-*N*-(trimethylsilyl)phenylalaninate (1.51 g, 4.88 mmol) was added in a single portion at −30 °C to a stirred solution of tri(cyanato-*N*)methylsilane (413 mg, 2.44 mmol) in acetonitrile (10 mL), and the mixture was then kept undisturbed at −20 °C for 10 d. The resulting colorless crystalline solid was isolated by filtration, washed with cold (0 °C) *n*-pentane (2×10 mL), and dried in vacuo (0.1 mbar, 60 °C, 8 h); yield, 429 mg (1.16 mmol, 48 %). M.p. >368 °C (decomp). The following NMR data refer to two crystallographically independent molecules: ^{13}C VACP/MAS NMR: δ = 1.8 ($SiCH_3$), 34.7 (CH_2), 38.2 (CH_2), 43.1 (CH_2), 45.7 (CH_2), 54.6 (br asymmetric "d"; CH),[16] 56.0 (br asymmetric "d"; CH),[16] 57.1 (br asymmetric "d"; CH),[16] 59.5 (br asymmetric "d"; CH),[16] 126.1, 126.5, 127.3, 127.6, 128.8, 129.5, 130.4, 131.4, 135.3, 135.7, 136.6, and 139.1 (C_6H_5), 172.4 (CO), 173.3 (CO), 179.0 ppm (2 CO); ^{15}N VACP/MAS NMR: δ = −332.2 (2N, NH or NH_2), −323.1 (NH or NH_2), −321.2 ppm (NH or NH_2); ^{29}Si VACP/MAS NMR: δ = −87.9 (br asymmetric "d"),[16] −85.5 ppm (br asymmetric "d");[16] elemental analysis calcd (%) for $C_{19}H_{22}N_2O_4Si$ (370.48): C 61.60, H 5.99, N 7.56; found: C 61.3, H 6.0, N 7.7.

Synthesis of 10: Trimethylsilyl (*S*)-*N*-(trimethylsilyl)phenylalaninate (1.58 g, 5.10 mmol) was added in a single portion at −70 °C to a stirred solution of tri(cyanato-*N*)phenylsilane (590 mg, 2.55 mmol) in acetonitrile (11 mL), and the mixture was then kept undisturbed at −20 °C for 3 d. The resulting colorless crystalline solid was isolated by filtration, washed with cold (0 °C) *n*-pentane (3×10 mL), and dried in vacuo (0.8 mbar, 23 °C, 24 h); yield, 628 mg (1.45 mmol, 57 %). M.p. >320 °C (decomp). The following solution NMR data refer to two isomers (molar ratio **A**:**B**, ca. 1:1.3): ^{1}H NMR (c = 72 mM): δ = 2.51–3.24 (m, 4H; CH_2, **A** and **B**), 2.89 (**A**) and 2.95 (**B**) (2d, $^3J \approx 1.7$ Hz, 1H; NH, **A** and **B**), 3.53–3.94 (m, 2H; CH, **A** and **B**), 5.11 (t, J = 11.0 Hz; **B**), 5.50 (dd, J = 12.0, J = 9.2 Hz, **A**), and 6.05–6.11 (m, 2H; NH_2, **A** and **B**), 7.14–7.43 ppm (m, 15H; C_6H_5, **A** and **B**); ^{13}C NMR (c = 72 mM): δ = 34.9/41.54 (CH_2, **B**), 36.1/41.48 (CH_2, **A**), 54.4/57.2 (CH, **A**), 55.4/56.7 (CH, **B**), 126.2, 126.3, 126.6, 126.7, 126.8, 127.5, 127.6, 128.07, 128.09, 128.26, 128.33, 128.36, 128.44, 128.6, 128.7, 129.1, 129.15, 129.18, 129.4, 129.5, 131.8, 132.6, 136.6, 138.4, 137.3, 138.3, 138.6, and 139.6 (C_6H_5, **A** and **B**), 170.5/174.4 (CO, **B**), 171.2/174.5 ppm (CO, **A**); ^{15}N NMR (50.7 MHz; c, 72 mM): δ = −340.5 (NH, **B**), −337.4 (NH, **A**), −327.9 (NH_2, **B**), −326.8 ppm (NH_2, **A**); ^{29}Si NMR (c = 72 mM): δ = −99.1 (**B**), −97.7 ppm (**A**); ^{13}C VACP/MAS NMR: δ = 32.9 (CH_2), 40.1 (CH_2), 54.2 (br asymmetric "d"; CH),[16] 57.9 (asymmetric "d"; CH),[16] 127.3, 127.6, 127.8, 128.4, 129.2, 130.2, 130.6, 133.0, 134.7, and 137.7 (C_6H_5), 168.9 (CO), 181.2 ppm (CO); ^{15}N VACP/MAS NMR: δ = −334.0 (NH), −324.4 ppm (NH_2); ^{29}Si VACP/MAS NMR: δ = −98.5 ppm (br asymmetric "d");[16] elemental analysis calcd (%) for $C_{24}H_{24}N_2O_4Si$ (432.55): C 66.64, H 5.59, N 6.48; found: C 66.3, H 5.5, N 6.6.

Synthesis of 11: Trimethylsilyl (*S*)-*N*-trimethylsilyl)leucinate (1.50 g, 5.44 mmol) was added in a single portion at −45 °C to a stirred solution of tri(cyanato-*N*)phenylsilane (610 mg, 2.64 mmol) in acetonitrile (20 mL), and the mixture was held at −45 °C for 5 min, layered with *n*-pentane (15 mL), and then kept undisturbed at −20 °C for 20 d. The resulting colorless crystalline solid was isolated by filtration, washed with cold (0 °C) *n*-pentane (2×10 mL), and dried in vacuo (0.8 mbar, 60 °C, 14 h); yield, 468 mg (1.28 mmol, 49 %). M.p. 241 °C (subl); ^{13}C VACP/MAS NMR: δ = 28.2 ($C(CH_3)_3$), 34.8 ($C(CH_3)_3$), 37.4 ($C(CH_3)_3$), 65.8 (br asymmetric "d"; CH),[16] 128.4, 129.0, 130.8, 137.3 and 138.7 (C_6H_5), 171.6 (CO), 179.4 ppm (CO), resonance signals for *n*-pentane and acetonitrile not detected; ^{15}N VACP/MAS NMR: δ = −339.2 (NH or NH_2), −328.8 ppm (NH or NH_2); ^{29}Si VACP/MAS NMR: δ = −92.3 ppm (br "s");[16] elemental analysis calcd (%) for $C_{18}H_{28}N_2O_4Si$ (364.52): C 59.31, H 7.74, N 7.69; found: C 58.7, H 7.8, N 7.7.

Crystal structure analyses: Suitable single crystals of **6**, **7**, **8**·CH_3CN, **9**, **10**, and **11**·C_5H_{12}·0.5 CH_3CN were obtained directly from the respective reaction mixtures (see the Synthesis section). The crystals were mounted in inert oil (perfluoropolyalkyl ether, ABCR) on a glass fiber and then transferred to the cold nitrogen gas stream of the diffractometer (Stoe IPDS (**7**, **8**·CH_3CN, **9**; graphite-monochromated $Mo_{K\alpha}$ radiation, λ = 0.71073 Å); Bruker Nonius KAPPA APEX II (**6**, **10**, and **11**·C_5H_{12}·0.5 CH_3CN; Montel mirror, $Mo_{K\alpha}$ radiation, λ = 0.71073 Å)). All structures were solved by direct methods (SHELXS-97).[17] The non-hydrogen atoms were refined anisotropically (SHELXL-97).[17] For the CH hydrogen atoms, a riding model was employed, whereas the NH hydrogen atoms were localized in the difference Fourier syntheses and refined freely. CCDC-757738 (**6**), 757739 (**7**), 757740 (**8**·CH_3CN), 757741 (**9**), 757742 (**10**), and 757743 (**11**·C_5H_{12}·0.5 CH_3CN) contain the supplementary crystallographic data for this paper. These data can be obtained free of charge from The Cambridge Crystallographic Data Centre via www.ccdc.cam.ac.uk/data_request/cif.

---

[1] For selected reviews dealing with higher-coordinate silicon compounds, see: a) R. R. Holmes, *Chem. Rev.* **1996**, *96*, 927–950; b) D. Kost, I. Kalikhman in *The Chemistry of Organic Silicon Compounds, Vol. 2, Part 2* (Eds.: Z. Rappoport, Y. Apeloig), Wiley, New York, **1998**, pp. 1339–1445; c) V. Pestunovich, S. Kirpichenko, M. Voronkov in *The Chemistry of Organic Silicon Compounds, Vol. 2, Part 2* (Eds.: Z. Rappoport, Y. Apeloig), Wiley, Chichester, **1998**, pp. 1447–1537; d) C. Chuit, R. J. P. Corriu, C. Reyé in *Chemistry of Hypervalent Compounds* (Ed.: K.-y. Akiba), Wiley-VCH, New York, **1999**, pp. 81–146; e) R. Tacke, M. Pülm, B. Wagner, *Adv. Organomet. Chem.* **1999**, *44*, 221–273; f) M. A. Brook, *Silicon in Organic, Organometallic, and Polymer Chemistry*, Wiley, New York, **2000**, pp. 97–114; g) R. Tacke, O. Seiler in *Silicon Chemistry: From*

the Atom to Extended Systems (Eds.: P. Jutzi, U. Schubert), Wiley-VCH, Weinheim, **2003**, pp. 324–337; h) D. Kost, I. Kalikhman, *Adv. Organomet. Chem.* **2004**, *50*, 1–106; i) D. Kost, I. Kalikhman, *Acc. Chem. Res.* **2009**, *42*, 303–314.

[2] R. Tacke, R. Bertermann, C. Burschka, S. Dragota, M. Penka, I. Richter, *J. Am. Chem. Soc.* **2004**, *126*, 14493–14505.

[3] S. Dragota, R. Bertermann, C. Burschka, M. Penka, R. Tacke, *Organometallics* **2005**, *24*, 5560–5568.

[4] R. Bertermann, A. Biller, M. Kaupp, M. Penka, O. Seiler, R. Tacke, *Organometallics* **2003**, *22*, 4104–4110.

[5] a) B. Theis, S. Metz, F. Back, C. Burschka, R. Tacke, *Z. Anorg. Allg. Chem.* **2009**, *635*, 1306–1312; b) S. Metz, C. Burschka, R. Tacke, *Chem. Asian J.* **2009**, *4*, 581–586; c) S. Metz, C. Burschka, R. Tacke, *Organometallics* **2009**, *28*, 2311–2317; d) B. Theis, S. Metz, C. Burschka, R. Bertermann, S. Maisch, R. Tacke, *Chem. Eur. J.* **2009**, *15*, 7329–7338.

[6] a) S. Y. Bylikin, A. G. Shipov, E. P. Kramarova, V. V. Negrebetsky, A. A. Korlyukov, Y. I. Baukov, M. B. Hursthouse, L. Male, A. R. Bassindale, P. G. Taylor, *J. Organomet. Chem.* **2009**, *694*, 244–248; b) A. R. Bassindale, D. J. Parker, P. G. Taylor, R. Turtle, *Z. Anorg. Allg. Chem.* **2009**, *635*, 1288–1294; c) I. Kalikhman, E. Kertsnus-Banchik, B. Gostevskii, N. Kocher, D. Stalke, D. Kost, *Organometallics* **2009**, *28*, 512–516; d) S. Yakubovich, B. Gostevskii, I. Kalikhman, D. Kost, *Organometallics* **2009**, *28*, 4126–4132; e) E. Kertsnus-Banchik, E. Sela, J. Wagler, I. Kalikhman, D. Kost, *Z. Anorg. Allg. Chem.* **2009**, *635*, 1321–1325; f) K. Lippe, D. Gerlach, E. Kroke, J. Wagler, *Organometallics* **2009**, *28*, 621–629; g) A. Kämpfe, E. Kroke, J. Wagler, *Eur. J. Inorg. Chem.* **2009**, 1027–1035; h) E. Brendler, T. Heine, A. F. Hill, J. Wagler, *Z. Anorg. Allg. Chem.* **2009**, *635*, 1300–1305; i) G. W. Fester, J. Wagler, E. Brendler, U. Böhme, D. Gerlach, E. Kroke, *J. Am. Chem. Soc.* **2009**, *131*, 6855–6864; j) R. Gericke, D. Gerlach, J. Wagler, *Organometallics* **2009**, *28*, 6831–6834; k) E. P. A. Couzijn, D. W. F. van den Engel, J. C. Slootweg, F. J. J. de Kanter, A. W. Ehlers, M. Schakel, K. Lammertsma, *J. Am. Chem. Soc.* **2009**, *131*, 3741–3751; l) E. P. A. Couzijn, J. C. Slootweg, A. W. Ehlers, K. Lammertsma, *Z. Anorg. Allg. Chem.* **2009**, *635*, 1273–1278; m) G. González-García, E. Álvarez, Á. Marcos-Fernández, J. A. Gutiérrez, *Inorg. Chem.* **2009**, *48*, 4231–4238; n) M. Yamamura, N. Kano, T. Kawashima, *Z. Anorg. Allg. Chem.* **2009**, *635*, 1295–1299; o) R. S. Ghadwal, S. S. Sen, H. W. Roesky, G. Tavcar, S. Merkel, D. Stalke, *Organometallics* **2009**, *28*, 6374–6377.

[7] R. G. Neville, J. J. McGee, in *Inorganic Syntheses, Vol. VIII* (Ed.: H. F. Holtzclaw, Jr.), McGraw-Hill, New York, **1966**, pp. 23–27.

[8] G. S. Forbes, H. H. Anderson, *J. Am. Chem. Soc.* **1948**, *70*, 1043–1044.

[9] L. Birkofer, A. Ritter, *Chem. Ber.* **1960**, *93*, 424–427.

[10] The Berry distortions and the hydrogen bonding systems were analyzed by using the program system PLATON: a) PLATON, A. L. Spek, University of Utrecht, Utrecht, **2008**; b) A. L. Spek, *J. Appl. Crystallogr.* **2003**, *36*, 7–13.

[11] a) R. Tacke, R. Bertermann, M. Penka, O. Seiler, *Z. Anorg. Allg. Chem.* **2003**, *629*, 2415–2420; b) O. Seiler, C. Burschka, M. Fischer, M. Penka, R. Tacke, *Inorg. Chem.* **2005**, *44*, 2337–2346; c) O. Seiler, C. Burschka, K. Götz, M. Kaupp, S. Metz, R. Tacke, *Z. Anorg. Allg. Chem.* **2007**, *633*, 2667–2670.

[12] a) R. Ahlrichs, M. Bär, M. Häser, H. Horn, C. Kölmel, *Chem. Phys. Lett.* **1989**, *162*, 165–169; b) O. Treutler, R. Ahlrichs, *J. Chem. Phys.* **1995**, *102*, 346–354; c) M. von Arnim, R. Ahlrichs, *J. Comput. Chem.* **1998**, *19*, 1746–1757.

[13] a) J. P. Perdew, *Phys. Rev. B* **1986**, *33*, 8822–8824; b) A. D. Becke, *Phys. Rev. A* **1988**, *38*, 3098–3100.

[14] A. Schäfer, H. Horn, R. Ahlrichs, *J. Chem. Phys.* **1992**, *97*, 2571–2577.

[15] S. Sripanyakorn, R. Jugdaohsingh, W. Dissayabutr, S. H. C. Anderson, R. P. H. Thompson, J. J. Powell, *Br. J. Nutr.* **2009**, *102*, 825–834, and references therein.

[16] The resonance signals for ^{13}C and ^{29}Si nuclei bonded directly to a quadrupolar nucleus, such as ^{14}N with a nuclear spin $I=1$, show residual dipolar coupling, which can not be removed under MAS conditions. For this reason, these resonance signals appear as broad asymmetric doublets. In this context, see: a) S. J. Opella, M. H. Frey, T. A. Cross, *J. Am. Chem. Soc.* **1979**, *101*, 5856–5857; b) J. G. Hexem, M. H. Frey, S. J. Opella, *J. Am. Chem. Soc.* **1981**, *103*, 224–226; c) J. Böhm, D. Fenzke, H. Pfeifer, *J. Magn. Res.* **1983**, *55*, 197–204; d) A. Olivieri, L. Frydman, M. Grasselli, L. Diaz, *Magnet. Reson. Chem.* **1988**, *26*, 615–618.

[17] G. M. Sheldrick, *Acta Crystallogr. Sect. A* **2008**, *64*, 112–122.

Received: February 3, 2010